Supplementary material for: Population dynamics of mutualism and intraspecific density dependence: how θ-logistic density dependence affects mutualistic positive feedback

1 Description

In the main manuscript text we cited three analyses that we wished to include as supplemental material. These analyses include

1. modeling per capita births and death rates as separate nonlinear functions, each with their own exponent,
2. allowing the two species to have different exponents from one another, and
3. modeling the commonly-used saturating functional response between mutualist partners.

These items are described in sections 3–5 below, following a brief presentation of the stability analysis in section 2.

2 Stability analysis

The Jacobian matrix of main text eq. (2) is,

$$J = \begin{bmatrix} r_1 - (\theta_1 + 1)\alpha_1 N_1^{\theta_1} + \beta_1 N_2 & \beta_1 N_1 \\ \beta_2 N_2 & r_2 - (\theta_2 + 1)\alpha_2 N_2^{\theta_2} + \beta_2 N_1 \end{bmatrix}. \tag{S.1}$$

At any interior equilibrium (i.e., with $N_1^*, N_2^* > 0$), $r_i - \alpha_i N_i^{\theta_i} + \beta_i N_j = 0$ for $i, j = 1, 2$. Thus, the Jacobian simplifies to,

$$J = \begin{bmatrix} -\theta_1 \alpha_1 N_1^{\theta_1} & \beta_1 N_1 \\ \beta_2 N_2 & -\theta_2 \alpha_2 N_2^{\theta_2} \end{bmatrix}, \tag{S.2}$$

whose trace is negative. Therefore, by the Routh-Hurwitz stability conditions, an interior equilibrium of this system will be stable as long as the determinant of this Jacobian is positive. This occurs when,

$$\frac{\alpha_1 \alpha_2}{\beta_1 \beta_2} > \frac{N_1^{*1-\theta_1} N_2^{*1-\theta_2}}{\theta_1 \theta_2}. \tag{S.3}$$

Although we cannot simplify the stability conditions further for $\theta_i \neq 1$, eq. S.3 suggest that stability should be easier to achieve when the β_i are small and the θ_i are large. This is consistent with our numerical results in main text Fig. 2.

3 Independent births and deaths

3.1 Methods

In the main text, we relaxed the assumption that the difference between per capita birth and death rates decreased linearly as density increased. In this section, we assume that per capita birth and

death rates independently change as responses to density by modeling them as separate functions. To do this, we write each birth and death function as a density independent term, b_i or d_i, with a density dependent term, $\mu_i N_i^{\eta_i}$ or $\nu_i N_i^{\theta_i}$. Similar to the main text, the exponents cause the per capita birth or death rates to be a decelerating function of density if the exponent is < 1 and an accelerating function if the exponent is > 1 (Fig. S1). An exponent of 0 yields a density independent function were neither rate changes as a function of density.

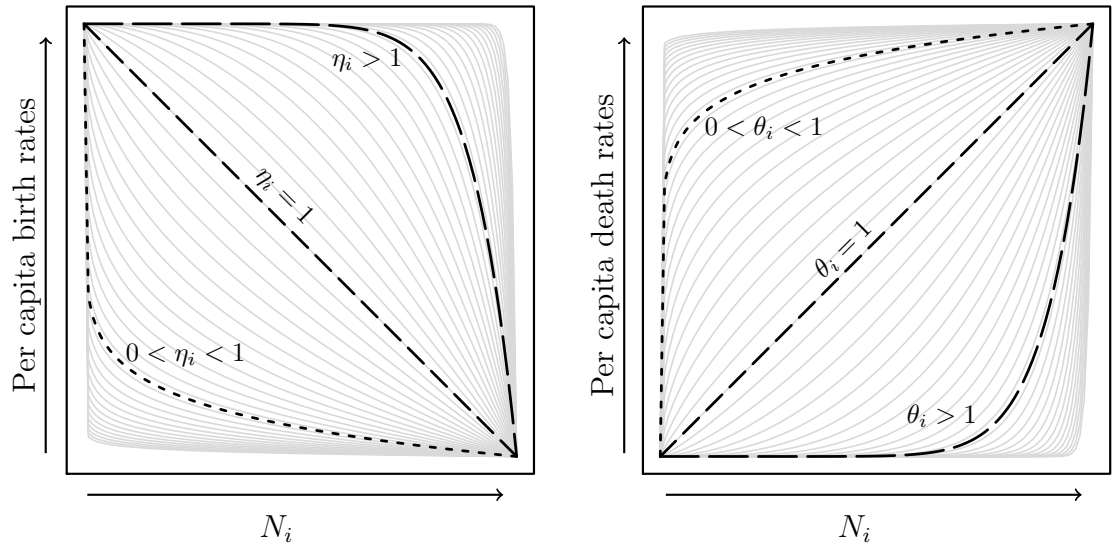

Figure S1: Values of η_i and θ_i used in eqs. (S.5) to represent nonlinear per capita birth and death rates before accounting for the effects of mutualism. Panels show how the per capita birth (left) and death (right) rates change as functions of intraspecific density, N_i. The actual values used for numerical analyses are presented in light gray, with highlighted examples of decelerating intraspecific density dependence (η_i or $\theta_i = 1/10$; short dashes, - - - - -), linear intraspecific density dependence (η_i or $\theta_i = 1$; medium dashes, — — —), and accelerating intraspecific density dependence (η_i or $\theta_i = 10$; long dashes, ——).

Pairing the per capita birth and death functions with a linear functional response, we arrive at

$$\begin{aligned} \frac{1}{N_1}\frac{dN_1}{dt} &= \left(b_1 - \mu_1 N_1^{\eta_1}\right) - \left(d_1 + \nu_1 N_1^{\theta_1}\right) + \beta_1 N_2 \\ \frac{1}{N_2}\frac{dN_2}{dt} &= \left(b_2 - \mu_2 N_2^{\eta_2}\right) - \left(d_2 + \nu_2 N_2^{\theta_2}\right) + \beta_2 N_1. \end{aligned} \tag{S.4}$$

Rearranged to group the density independent, density dependent, and mutualism terms, our model with a linear functional response is

$$\begin{aligned} \frac{1}{N_1}\frac{dN_1}{dt} &= (b_1 - d_1) - \left(\mu_1 N_1^{\eta_1} + \nu_1 N_1^{\theta_1}\right) + \beta_1 N_2 \\ \frac{1}{N_2}\frac{dN_2}{dt} &= (b_2 - d_2) - \left(\mu_2 N_2^{\eta_2} + \nu_2 N_2^{\theta_2}\right) + \beta_2 N_1. \end{aligned} \tag{S.5}$$

Fig. S2 shows the pairwise combinations between per capita birth and death rates of the four types of density dependence (independent, decelerating, linear, and accelerating) used in this section. An important comparison with the main text is that when per capita birth and death rates are equal (i.e., $\eta_i = \theta_i$), we recover the θ-logistic equation that we analyzed in the main text (roughly, the diagonal panels in Fig. S2). The results presented in this section therefore only consider when per capita birth and death rates are not equal (i.e., $\eta_i \neq \theta_i$).

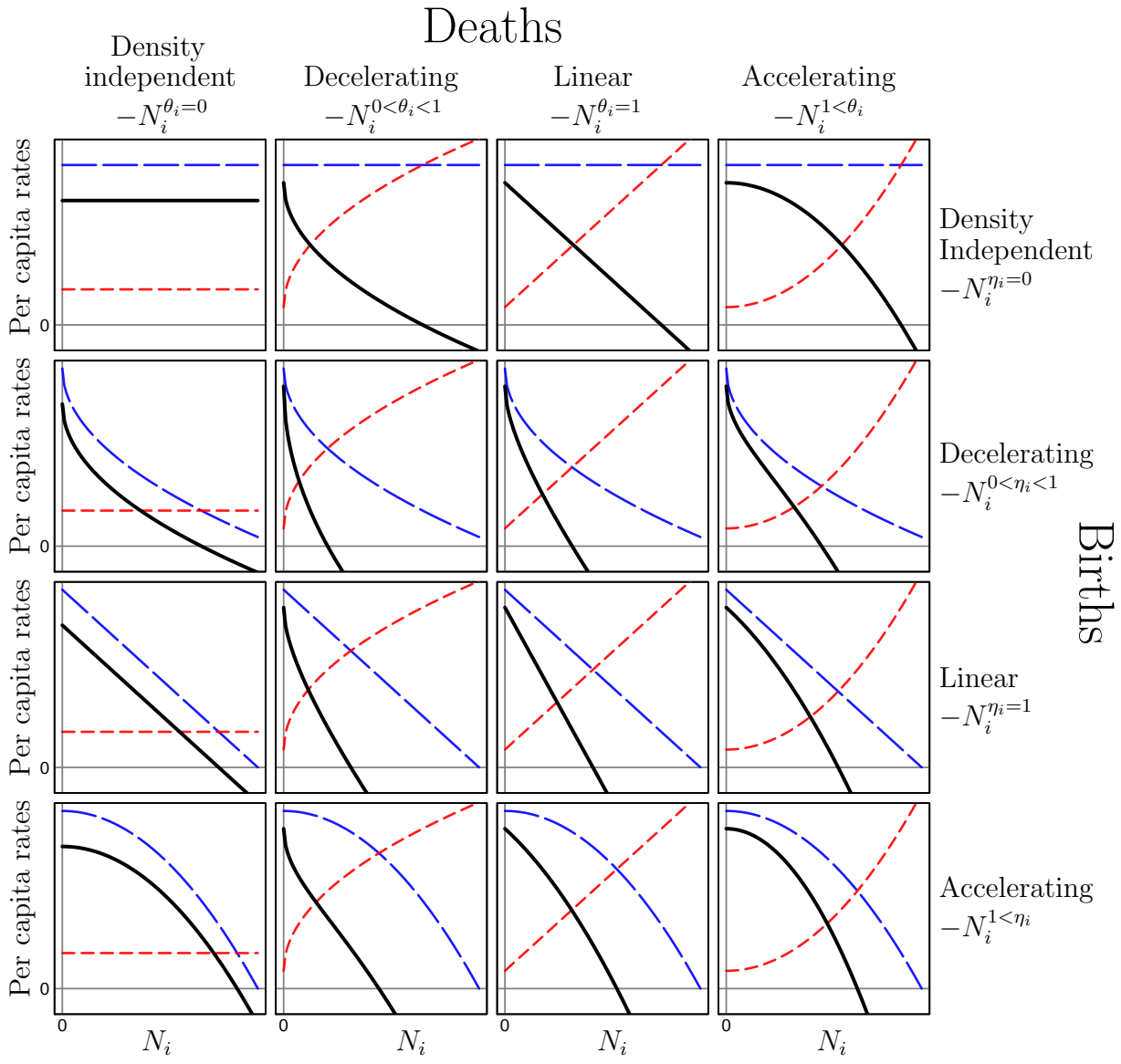

Figure S2: The qualitative range of per capita birth and death functions used to examine how relaxing the assumption of linear per capita intraspecific density dependence could affect the population dynamics of mutualism. Each panel's x-axis is population density, N_i, and the y-axis is the per capita birth, death, or growth rate. Per capita birth (— — —) and death (- - - -) rates respectively increase or decrease as a function of density. Across rows of panels the shape of density dependent births changes as η_i increases and across columns of panels the shape of density dependent deaths changes as θ_i increases. The difference between the birth and death rates, the per capita population growth rate (———), is superimposed to show that similar overall population growth functions can arise from different birth and death processes.

3.2 Results

When $\eta_i \neq \theta_i$, we found no dynamics qualitatively different from what we found in the main text when $\eta_i = \theta_i$. When either of the birth or death functions were density independent ($\eta_i = 0$ or $\theta_i = 0$), the population growth rates and model dynamics behaved according to the function without the non-zero exponent. Further, when either of the birth or death functions responded linearly to density, or both of the birth and death functions responded at a decelerating rate, the population growth rates and model dynamics were behaved similarly to cases with decelerating density dependence (Fig. S3, $\eta_i \leq 1$ and $\theta_i \leq 1$).

There was one important difference when we modeled per capita birth and death rates independently. Specifically, if either of the birth and death functions were accelerating, then there was always one interior stable equilibrium (Fig. S3, $\eta_i > 1$ and $\theta_i > 1$). This finding is irrespective of the strength of mutualism.

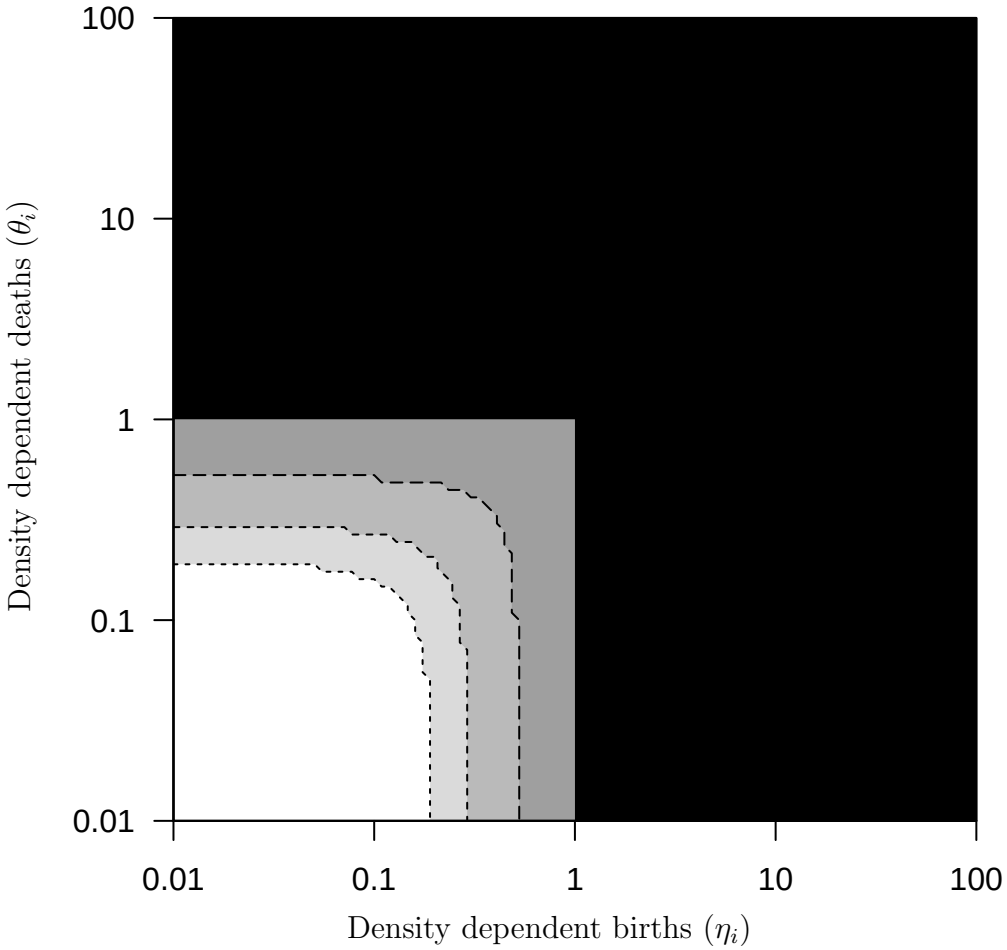

Figure S3: Number of equilibrium points given independent per capita birth (η_i; x-axis) and death (θ_i; y-axis) functions, for different strengths of a linear mutualism functional response (β_i; grayscale). If either birth (η_i) or death (θ_i) functions were accelerating (> 1), then there was always one interior equilibrium and it was stable (black), irrespective of the strength of mutualism (β_i). We only show parameter space up to 10^2, but a stable interior equilibrium was present for any value greater than 1. If both birth and death functions were decelerating (< 1), then the strength of mutualism determined if there was no interior equilibrium or two interior equilibria. Contours lines delineate the no-interior- (white) and two-interior-equilibrium (gray) boundaries for several strengths of mutualism (10^{-1} (— —, darkest gray), 10^{-2} (– –, medium gray), and 10^{-3} (- - -, lightest gray)).

4 Different exponents between species

4.1 Methods and results

In the main text we examined the effect of nonlinear intraspecific density dependence on the population dynamics of a pair of mutualists. One assumption we made was that the type of intraspecific density dependence was the same for both species; i.e., we assumed $\theta_i = \theta_j$. In this section we relax this assumption so that $\theta_i \neq \theta_j$, and analyzed the model in the same way as in the main text (numerically and graphically).

When $\theta_i \neq \theta_j$, we found no dynamics qualitatively different from what we found in the main text (Fig. S4). That is, depending on the values of θ_i and θ_j, we found between 3 and 5 non-negative equilibrium population sizes. When $\theta_i = 1$ and $\theta_j < 1$, or vice versa, the model either has no interior equilibria and grows without bound, or two interior equilibria, with the point closest to the origin being stable (Fig. S4, left column). When $\theta_i = 1$ and $\theta_j > 1$, or vice versa, there was always a single, stable interior equilibrium point (Fig. S4, center column). When $\theta_i > 1$ and $\theta_j < 1$, or vice versa, the model has either one interior equilibrium, which is stable, or no interior equilibria and unbounded growth (Fig. S4, right column). Comparing Fig. S4 with Fig. 3 in the main text, we find broad consistency between these two versions of the model. When one species' θ value equals 1, the behavior of the model will be determined by the other exponent. That is, the two cases that are possible when $\theta_i = 1, \theta_j < 1$ in Fig. S4 match the two cases for $(\theta_i = \theta_j) < 1$ in the main text. Further, the single, stable interior equilibrium seen when $\theta_i = 1, \theta_j > 1$ matches the model's behavior when $(\theta_i = \theta_j) > 1$. Interestingly, mixing and matching $\theta_i < 1, \theta_j > 1$ yields two possible outcomes that match the two outcomes seen when $\theta_i = \theta_j = 1$.

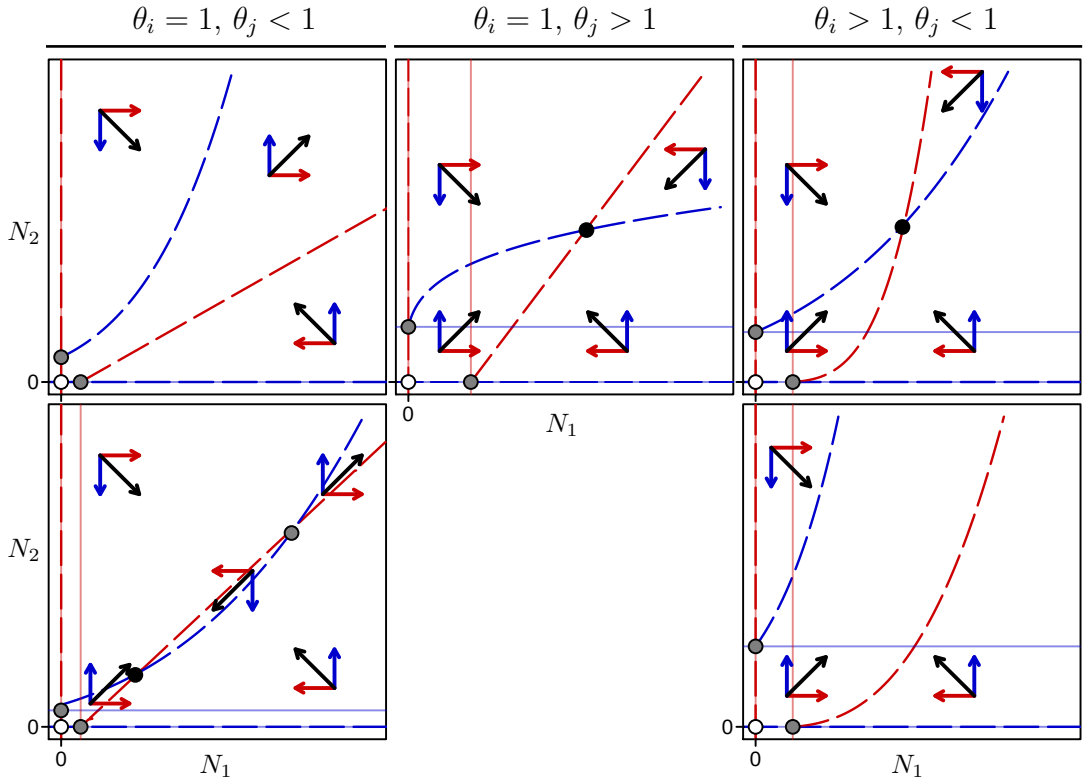

Figure S4: Phase planes representing the qualitative dynamics of 2-species mutualistic interactions for different models of per capita intraspecific density dependence between species. Each panel shows the densities of N_1 and N_2 on the x- and y-axes. Within each panel, zero-growth isoclines (nullclines) are shown for N_1 (red) and N_2 (blue): (i) when there is no mutualism ($\beta_i = 0$) as solid, light lines (—— or ——) and (ii) when mutualism is present ($\beta_i > 0$) as dashed lines (— — or — —). Arrows within panels show the qualitative direction vectors for N_1 (red), N_2 (blue), and together (black) for all changes in direction for each phase plane. Points within panels represent unstable (white), stable (black), or saddle nodes (gray).The columns show the five qualitative different outcomes when $\theta_i \neq \theta_j$, with the left column being $\theta_i = 1$ and $\theta_j < 1$, the center column being $\theta_i = 1$ and $\theta_j > 1$, and the right column being $\theta_i > 1$ and $\theta_j < 1$.

5 Saturating functional response

5.1 Methods

To more fully understand the effect of relaxing the assumption of linear intraspecific density dependence, we extend our approach to include a saturating functional response. Specifically, we replace the $\beta_i N_j$ in eq. 2 from the main text with a saturating function (following Wright, 1989; Holland et al., 2002; Holland and DeAngelis, 2010, and others), to create equations:

$$\begin{aligned} \frac{1}{N_1}\frac{dN_1}{dt} &= r_1 - \alpha_1 N_1^{\theta_1} + \frac{\gamma_1 N_2}{\delta_1 + N_2} \\ \frac{1}{N_2}\frac{dN_2}{dt} &= r_2 - \alpha_2 N_2^{\theta_2} + \frac{\gamma_2 N_1}{\delta_2 + N_1}, \end{aligned} \tag{S.6}$$

with γ_i being the maximum benefit species j can confer to species i and δ_i as the half-saturation constant, which controls how quickly the saturation of benefits occurs. For a more mechanistic, consumer-resource-based interpretation of the parameters in the saturating functional response for mutualisms, see Revilla (2015).

5.2 Results

In general, our findings with respect to the benefit of mutualism were the same: as intraspecific density dependence shifted from decelerating to accelerating, for a given strength of mutualism (γ_i is roughly analogous to β_i in the linear functional response), the benefit of mutualism decreased (Fig. S5, right panel). Also, increasing the strength of mutualism (γ_i) always increased the benefit of mutualism for any type of density dependence. There were three major differences between the linear and saturating models. First, in the saturating model, there were no unstable configurations (Fig. 4 from the main text, center panel, compared with Fig. S5, center panel). Second, again in the saturating model, across all values of strength of mutualism and density dependence there were always four equilibria, with a single, stable interior equilibrium. Third, weak accelerating density dependence with a linear functional response produced a disproportionally large spike in benefit from mutualism (Fig. 4 from the main text, right panel, compared with Fig. S5, right panel).

5.3 Discussion

We compared both linear and saturating functional responses because the latter response is now widely used as an alternative that prevents unrealistic outcomes of the Lotka-Volterra mutualism model (e.g., Holland et al., 2002, 2006; Okuyama and Holland, 2008; Holland and DeAngelis, 2010; Bastolla et al., 2009; Rohr et al., 2014; Pascual-García and Bastolla, 2017). The effects of nonlinear per capita intraspecific density dependence was largely the same for both models, with the mutualistic benefit being greatest with decelerating density dependence. We postulate that this is a general phenomenon that we expect to see with other types of mutualistic functional responses. As an example, in a hypothetical seed-caching seed-dispersal mutualism, we can expect that the per capita effect of the seed-caching animals on the nut-producing plants will be constant; i.e., seed-caching animals disperse all nuts, regardless of the density of seed-caching animals. In this case, we may model the functional response as a constant function $g_i(N_j) = \epsilon_i$, with ϵ_i being the constant per capita benefit of having any amount of seed-caching animals present. Coincidentally, this example is actually a special case of to the saturating functional response, as the upper limit of the saturating function as $N_j \to \infty$ or $\delta_i \to 0$ is a constant (ϵ_i would equal γ_i in eq. (S.6)).

The two major differences between the dynamics of our models with linear and saturating functional responses were (i) the saturating functional response model always had a stable interior equilibrium and (ii) there was a strong peak in the population densities with weak accelerating density dependence with a linear functional response that was not present with a saturating functional response (Fig. 4 from the main text, center and right panels). Unlike the linear functional response, the model with a saturating functional response withstood destabilization with linear and

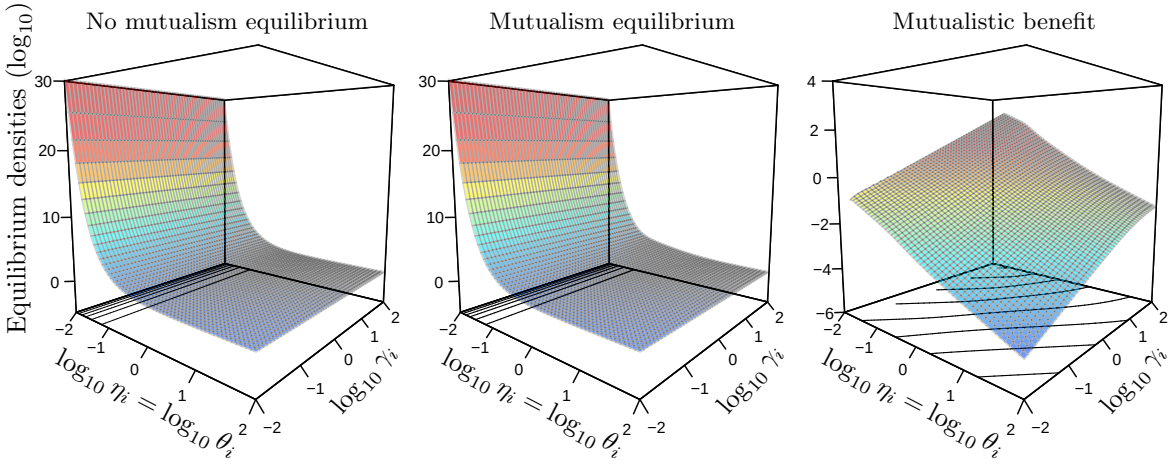

Figure S5: For model (S.6), nonlinear per capita growth rates with a saturating functional response of mutualism, the location of the interior equilibrium in the absence of mutualism (left), stable interior equilibrium with mutualism (center), and the benefit of mutualism, as the difference between the two (right). The locations of equilibria were identified as the Euclidean distance from the origin, $\sqrt{(N_i^*)^2 + (N_j^*)^2}$, for identical parameters for each species: $r_i = 4$, $\alpha_i = 2$. Each panel shows the aforementioned response on the vertical axis, the type of intraspecific density dependence (θ_i from 10^{-2}–10^2) on the left horizontal axis, and the strength of mutualism (γ_i from 10^{-2}–10^2) on the right horizontal axis. Further, each panel shows the relative values of each surface (colors), the absolute values of each surface (same axes across panels), and contour lines at the base of each plot show changes in the surface.

decelerating density dependence when relatively strong mutualism was added. Indeed, persistent stabilization is one of the most attractive features of the saturating functional response. Although it remained stable with stronger deceleration, we found that the mutualistic benefit continued to increase, which does not seem to be a realistic feature of our models. The peak in the mutualistic benefit in the model with a linear functional response was the other difference compared with the saturating functional response model, which also does not seem to be a realistic feature. This peak arose from parameter space where accelerating density dependence was weak and the strength of the linear functional response was strong (for $1 < \eta_i$ or $\theta_i < 2$). We did not observe a similar peak in the models with a saturating functional response because at higher densities the benefit of the mutualism is diminished.

References

Bastolla, U., Fortuna, M. A., Pascual-Garcia, A., Ferrera, A., Luque, B., Bascompte, J., 04 2009. The architecture of mutualistic networks minimizes competition and increases biodiversity. Nature 458 (7241), 1018–1020.

Holland, J. N., DeAngelis, D. L., May 2010. A consumer-resource approach to the density-dependent population dynamics of mutualism. Ecology 91 (5), 1286–1295.

Holland, J. N., DeAngelis, D. L., Bronstein, J. L., Mar 2002. Population dynamics and mutualism: Functional responses of benefits and costs. American Naturalist 159 (3), 231–244.

Holland, J. N., Okuyama, T., DeAngelis, D. L., 09 2006. Comment on "Asymmetric coevolutionary networks facilitate biodiversity maintenance". Science 313 (5795), 1887b.

Okuyama, T., Holland, J. N., 2008. Network structural properties mediate the stability of mutualistic communities. Ecology Letters 11 (3), 208–216.

Pascual-García, A., Bastolla, U., 02 2017. Mutualism supports biodiversity when the direct competition is weak. Nature Communications 8, 14326 EP –.
URL http://dx.doi.org/10.1038/ncomms14326

Revilla, T. A., Aug 2015. Numerical responses in resource-based mutualisms: A time scale approach. Journal of Theoretical Biology 378, 39–46.

Rohr, R. P., Saavedra, S., Bascompte, J., 07 2014. On the structural stability of mutualistic systems. Science 345 (6195).

Wright, D. H., 1989. A simple, stable model of mutualism incorporating handling time. American Naturalist 134 (4), 664–667.